Precipitation and Dissolution of Solids Attending Flow through Porous Media

A model is developed that calculates the chemical equilibrium that exists between a flowing electrolyte solution and mineral assemblages. The development computes the mineral and aqueous compositions as a function of time and position in a one-dimensional porous medium. The model considers the dissolution of solids as well as their precipitation. The application of the model to various problems has revealed that characteristic aqueous and solid phase concentration waves develop and propagate through the system in a chromatographic manner. Example calculations are presented that illustrate the widespread applicability of the model. Specifically, a calculation is presented that reproduces the genetic mineralization features that are found in sandstone-type uranium deposits.

M. P. WALSH, S. L. BRYANT, R. S. SCHECHTER, and L. W. LAKE

The University of Texas at Austin
Department of Petroleum Engineering
Austin, TX 78712

SCOPE

Porous sedimentary formations are composed of a variety of minerals ranging from highly abundant species, such as carbonates, clays, feldspars, and quartz, to trace compounds containing valuable elements such as uranium, vanadium, silver and copper. When reactive fluids are introduced into these formations, the minerals can dissolve and, once mobilized, mix with the injected fluids. Precipitates may form from the resulting mixture. Knowing how fast mineral phases form and transport is of critical importance to caustic flooding (DeZabala et al., 1982; Ehrlich and Wygal, 1977; Bunge and Radke, 1981), micellar/polymer flooding (Hill and Lake, 1978; Somasundran et al., 1979; Hirasaki, 1982), steam flooding (Reed, 1980), sandstone acidizing (Labrid, 1975; Shaughnessy and Kunze, 1981; Smith and Hendrickson, 1965), near wellbore scaling (Vetter and Kandarpa, 1980; Read and Ringen, 1982), and mineral leaching (Tatom et al., 1981; Gao et al., 1981).

General methods which describe dissolution and precipitation of solids attending flow have not been developed. Sophisticated models for specific applications have been reported (Hekim et al., 1982; Hekim and Fogler, 1980); however, their general use is limited by the availability of suitable kinetic data. To overcome these difficulties, we use chemical equilibrium to develop a general predictive method, utilizing the vast resources of published thermodynamic data.

In recent years several equilibrium geochemical models of batch systems have been reported which can be divided into two broad classes. The first class consists of those which accept overall solution concentrations of elements, speciate them, and identify supersaturated minerals (Plummer et al., 1976; Kharaka and Barnes, 1973). No attempt is made to quantify the amount of precipitate. A more sophisticated class of batch geochemical models does quantify precipitation and mineral dissolution (Westall et al., 1976; Wolery, 1979; Helgeson et al., 1970; Parkhurst et al., 1980). As shown in Table 1, these equilibrium models do not consider hydrodynamic flow.

Presented here is a general geochemical simulator which does include flow based on the equilibrium approach. The model assumes chemical equilibrium between an aqueous solution flowing in a linear, one-dimensional porous medium, and solves for the mineral and aqueous-phase compositions as a function of both time and position. Included are the dissolution and precipitation of minerals, oxidation-reduction reactions, and adsorption. The computer program is a complex one and only an outline of the numerical procedure is given here; but some unexpected general features of the problem have emerged and these are detailed.

CONCLUSIONS AND SIGNIFICANCE

The application of the geochemical simulator to specific problems revealed that characteristic concentration waves (both solid and aqueous phases) develop and move through the system in a manner reminiscent of the chromatographic movement of gases or liquids. The structure of these waves has been studied and three essential features identified. One is the mineral sequence that defines the order of the mineral phases which exist, beginning at the injection point and ending at a point in the porous medium occupied by the minerals at their initial concentration. The identification of the mineral sequence is only generally possible using the computer simulator.

The second feature is coherence, a condition that requires the concentration velocity of all elements in a wave to be equal. Coherence leads to an important result which will help to solve algebraically all problems having the same mineral sequence. Such problems have been termed scalable.

The last feature characterizing the waves is that the solution downstream of a solid which has disappeared across a wave must remain in equilibrium with that solid. This "downstream equilibrium condition" is required to algebraically solve scalable problems.

The concept of scalability is both interesting and practical. The geochemical simulator often requires large blocks of computer time to achieve a solution, whereas scalable problems require only one computer run to determine the mineral sequence, and subsequent problems are solved algebraically.

To illustrate the application of the simulator and of the scalability concept, we show several simple problems not involving oxidation-reduction reactions.

The simulator has also been applied to the deposition of uranium in roll front deposits. The model quantitatively reproduced typical ore grades and deposit ages and qualitatively showed that certain minerals, codeposited with uranium, occupy actually observed positions in the roll front. The predictions support the theory that uranium was originally mineralized in roll fronts when oxidized uranium-bearing groundwaters contacted highly reduced sandstones.

Correspondence concerning this paper should be directed to L. W. Lake.

TABLE 1. SOME EQUILIBRIUM MODELS AND THEIR FEATURES

	Activity Coefficient Correction	Evaluates Mineral Saturation Given Key Solution Phase Compositions	Finds Mineral Phase Compositions Given Overall Element Concentrations	Calculates Mineral Composition Given Overall Element Concentrations and Mineral Assemblage	Oxidation-Reduction (redox) Reactions Possible	Considers Nonequilibrium Mineral Dissolution (not in real time)	Mineral Adsorption	Batch Calculation	1-D Fluid Flow
WATEQF[1]	X	X							
SOLMNEQ[2]	X	X							
PHREEQE[3]	X	X		X	X			X	
EQ3/EQ6[4]	X	X	X	X	X	X		X	
PATHI[5]	X	X	X	X	X	X		X	
MINEQL[6]	X	X	X	X				X	
MINEQL1+STANFORD[7]	X	X	X	X			X	X	
PHASEQL/FLOW*	X	X	X	X	X		X	X	X

* Model used for this paper.
[1] Plummer et al., 1976.
[2] Kharaka et al., 1973.
[3] Parkhurst et al., 1980.
[4] Wolery, 1979.
[5] Helgeson et al., 1970.
[6] Westall et al., 1976.
[7] Davis et al., 1978.

MATHEMATICAL DEVELOPMENT OF FLOW WITH CHEMICAL EQUILIBRIA

Assumptions

When reactive fluids are introduced into porous formations many of the minerals originally present will dissolve and produce a new composition of water-soluble species. Under certain conditions of temperature and composition, the solubility of a new chemical species can be exceeded and result in the precipitation of a new solid. These precipitates can redissolve when contacted by a fluid of different composition. If the rate at which a solid dissolves is sufficiently fast, the reaction may be well approximated by assuming local thermodynamic equilibrium. The computation of this equilibrium in flowing electrolyte solutions can be accomplished through equilibria relationships, mass, charge, and electron balances. To simplify the formulation, the following idealizations and assumptions have been adopted.

(1) The system is one dimensional and the porous medium is homogeneous and isothermal with constant porosity.

(2) There is only one fluid phase whose density and viscosity is independent of composition.

(3) Fluid and solid phases are incompressible and in chemical equilibrium.

(4) There is no supersaturation of aqueous species.

(5) There is no flow or migration of solid mineral species.

Mass Balances

Subject to the above assumptions, if J is the total number of aqueous species present in the system and I is the total number of elements, excepting hydrogen and oxygen, the mass balance for element i is

$$\frac{\partial(\phi C_i^T)}{\partial t} + u\frac{\partial}{\partial x}\left(\sum_{j=1}^{J} h_{ij}C_j\right) - \frac{\partial^2}{\partial x^2}\left(\sum_{j=1}^{J}\phi K_{lj}h_{ij}C_j\right) = 0, \quad i = 1, \ldots, I \tag{1}$$

where

C_i^T = total or overall concentration of element i ($i = 1, \ldots, I$)
C_j = concentration of species j in aqueous phase ($j = 1, \ldots, J$)
h_{ij} = aqueous phase stoichiometric constant, the number of elements i in species j

The remaining terms in Eq. 1 are defined in the nomenclature.

The overall concentration C_i^T, by definition, includes contributions from both the aqueous and K minerals in the solid phase.

$$C_i^T = \sum_{j=1}^{J} h_{ij}C_j + \sum_{k=1}^{K} g_{ik}\hat{C}_k, \quad i = 1, 2, \ldots, I \tag{2}$$

where

$\hat{C}_k$ = concentration of mineral k ($k = 1, \ldots, K$)
g_{ik} = mineral phase stoichiometric constant, the number of elements i in mineral k

Note that, in accordance with assumption 5, there is no flux of solid-phase species in Eq. 1. This does not preclude the movement of precipitation waves through the medium as insoluble species can form whenever the appropriate solubility product is exceeded. Thus, we do not attempt to model the migration of dispersed particles (Khilar and Fogler, 1981).

To minimize the number of fluid flow parameters, the following dimenionless variables are introduced:

$$x_D = \frac{x}{L}, \quad t_D = \int_0^t \frac{u\,dt}{\phi L} \tag{3}$$

and used to cast Eq. 1 into

$$\frac{\partial}{\partial t_D}(C_i^T) + \frac{\partial}{\partial x_D}\left(\sum_{j=1}^{J} h_{ij}C_j\right) - \frac{1}{N_{Pe}}\frac{\partial^2}{\partial x_D^2}\left(\sum_{j=1}^{J} h_{ij}C_j\right) = 0, \quad i = 1, \ldots, I \tag{4}$$

where

$$N_{Pe} = \text{Peclet number} = \frac{uL}{K_l\phi} \text{ and}$$

L is the total system length and t_D is the volume of fluid injected expressed as a fraction of the pore volume. In the definition of N_{Pe}, the longitudinal dispersion coefficient has been taken to be equal for all aqueous species since macroscopic dispersion (species-independent) is usually greater than molecular diffusion. Equations 2 and 4, therefore, represent $2I$ equations with a maximum of $I + J + K$ unknowns (C_i^T, for $i = 1, \ldots, I$; C_j for $j = 1, \ldots, J$; and C_k for $k = 1, \ldots, K$) which require up to $J + K - I$ additional relations.

Electrical Neutrality

Inasmuch as the total concentration of hydrogen and oxygen greatly exceed all other elemental concentrations in the water of natural environments, we assume their total concentrations to be constant and invoke electrical neutrality to determine the hydrogen ion concentration (solution pH). The condition of electrical neutrality is:

$$\sum_{j=1}^{J} z_j C_j = 0 \tag{5}$$

where z_j is the charge of species j. Despite the convenience of this approach, the neglect of changes in total masses of hydrogen and oxygen can be misleading if large amounts of water are consumed during mineral precipitation. For example, one mole of mirabilite ($Na_2SO_4 \cdot 10\ H_2O$) precipitating from 1 L of solution removes 10 mol of H_2O from the aqueous phase with a resulting 20% increase in the concentration of the other constituents. Our model does not account for this change in concentration. However, we do consider the change in water activity with ionic strength and its effect on the chemical equilibria (Robinson and Stokes, 1959; Garrels and Christ, 1965).

Equilibrium Relations

An important consequence of a "fully" compositional (Pope and Nelson, 1978; Coats, 1980; Fleming et al., 1981; Lake et al., 1981) formulation is that once the I overall compositions are specified, the remaining unknowns (C_j for $j = 1, \ldots, J$ and $\hat{C}_k$ for $k = 1, \ldots, K$) may be determined from equilibrium relationships.

Any intraaqueous reaction may be written as

$$\sum_{j=1}^{J} \nu_{rj} S_j = 0, \quad r = 1, \ldots, R \tag{6}$$

where S_j is the chemical formula for species j and ν_{rj} is the stoichiometric coefficient for species j in reaction r ($\nu_{rj} < 0$ for reactants). The chemical equilibria between the products and reactants of the r^{th} intraaqueous reaction is:

$$K_r = \prod_{j=1}^{J} a_j^{\nu_{rj}}, \quad r = 1, \ldots, R \tag{7}$$

where K_r is the thermodynamic equilibrium constant and a_j is the chemical activity of aqueous species j. The equilibrium constant may be obtained from the free energies of formation of the products and reactants in their standard states. The chemical activities in Eq. 7 are related to molal concentrations through activity coefficients γ_j

$$a_j = \gamma_j C_j, \quad j = 1, \ldots, J \tag{8}$$

where the activity coefficient is activity coefficient relations (Robinson and Stokes, 1968; Lewis and Randall, 1923; Helgeson, 1969).

The chemical equilibria between the solid phase minerals and aqueous species, the second category of equilibria, can be similarly described using a mass action equation.

$$K_k^{sp} \geq \prod_{j=1}^{J} a_j^{\nu_{kj}}, \quad k = 1, \ldots, K \tag{9}$$

where K_k^{sp} is the equilibrium constant (solubility product) for mineral phase k. This equation assumes that the activity of the mineral phase is unity. The equal sign shown in Eq. 11 applies only if the solubility of the aqueous species exceeds the solubility product. Thus, to calculate the chemical equilibrium state of a system, all k solubility equations must be evaluated to determine whether or not they are exceeded. Furthermore, because more than one mineral may be present at a time, the correct assemblage of minerals must be determined. For use in our numerical approach, a scheme outlined by Morgan and Morel (1972) is implemented.

Electron Balance

Redox reactions are a class of chemical reactions involving elements which change oxidation states. Redox reactions can either be written as half-cell reactions or as reactions involving transfer of oxygen. To insure that all electrons donated by chemical species are correspondingly accepted by another, and hence, all half cells are balanced, we must invoke the conservation of electrons. This is entirely equivalent to the statement that oxidation numbers are conserved in a chemical reaction.

If we define ψ^T as the total concentration of available electrons, we can write

$$\phi \frac{\partial \psi^T}{\partial t} + u \frac{\partial \psi}{\partial x} - \phi K_l \frac{\partial^2 \psi}{\partial x^2} = 0 \tag{10}$$

where ψ is the concentration of available electrons in the aqueous phase. The overall concentration of available electrons, like the overall concentration of an element, consists of contributions from both the aqueous and solid phases

$$\psi^T = \psi + \hat{\psi} \tag{11}$$

where $\hat{\psi}$ is the concentration of available electrons in the solid phase. The quantities ψ and $\hat{\psi}$ are given by

$$\psi = \sum_{j=1}^{J} C_j \sum_{i=1}^{I} h_{ij}(P_i^M - P_{ij}) \tag{12}$$

$$\hat{\psi} = \sum_{k=1}^{K} C_k \sum_{i=1}^{I} g_{ik}(P_i^M - \hat{P}_{ik}) \tag{13}$$

where

P_i^M = valence of element i in its maximum oxidation state
P_{ij} = valence of element i in aqueous species j
$\hat{P}_{ik}$ = valence of element i in solid species k

In a nonredox system, the total concentration of the elements must first be determined before one can calculate the unknown aqueous and mineral species concentrations. In a redox system, both the total concentrations of elements and available electrons must first be known before speciation can be carried out. The unknowns in a redox problem are not only the aqueous and mineral species concentrations, but also a redox parameter which describes the oxidation status of the system. To remain consistent with our computational approach which uses concentrations or activities as the unknowns, the "activity of electrons" is used as the unknown redox parameter. This choice permits the definition of a reaction equilibrium constant for each redox half cell reaction.

Regardless of the redox parameter selected, once having determined one redox parameter, all others (for example, the oxidation potential Eh) can easily be calculated.

Numerical Solution

To solve the equations presented above, the flow equations (Eqs. 4 and 10) were transformed into an explicit, backwards in space, finite difference form. This technique allows physical dispersion to be approximated by numerical dispersion (Roache, 1976).

To solve the charge, electron, and element balances, Eqs. 2, 5 and 11, when chemical equilibria is imposed by the nonlinear relations in Eqs. 7 and 9, a standard Newton-Raphson (Carnahan et al., 1969) technique is employed. This technique has been shown to be adequate to solve the systems of equations commonly encountered in batch chemical equilibrium simulators (Westall et al., 1976; Helgeson et al., 1970; Wolery, 1978; Crear, 1975; I and Nancollas, 1972; Ingri et al., 1967; Perrin and Sayce, 1967; Bos and Meershoer, 1972; Zeleznik and Gordon, 1968). The Netwon-Raphson package is coupled with a direct search optimization algorithm (Himmelblau, 1972; Wood, 1960) to minimize convergence difficulties caused by poor initial root guesses. Also, because the roots to the nonlinear equations can vary over 30 orders of magnitude, the solution variables are transformed into a logarithmic form. This procedure, and the details of all the numerical techniques employed, can be found elsewhere (Walsh, 1983).

APPLICATION OF THE EQUILIBRIUM COMPOSITIONAL SIMULATOR

We apply our compositional flow simulator to two example problems:

(1) A simplified four-element flow problem where only one solid is dissolved by a reactive fluid.

(2) A uranium roll-front deposition problem which involves a

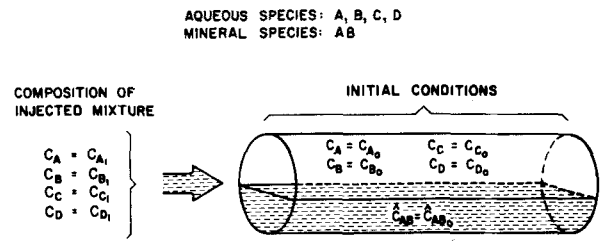

Figure 1. Simplified four-element flow problem.

system of more than 60 aqueous species and over 26 possible solids and which is additionally complicated by redox reactions. Examples involving sandstone acidizing are found elsewhere (Walsh et al., 1982).

The simple problem is presented for illustration and to introduce and establish some chromatographic concepts. The characteristic features of the simplified example, however, are the same as those in more complex problems.

Four Element Problem

In this example, we consider a porous medium which consists of an inert material containing solid $\overline{AB}$. Into the medium is injected a fluid consisting of three species: A, C and D (no B injected), Figure 1. The product of the initial solution concentrations of A and B must equal the $\overline{AB}$ solubility product. Since the injected fluid is devoid of species B, the mineral $\overline{AB}$ will dissolve as flow commences. Clearly, as the amount of mineral initially present and the concentrations of A and B in the injected solution increase, or, as the solubility product decreases, larger volumes will be required to dissolve $\overline{AB}$.

Figure 2a shows the results of a model calculation on a time-distance diagram where dimensionless distance, x_D, is plotted versus dimensionless time, t_D. On such a diagram, lines emanating from the origin are curves of constant composition (Helfferich and Klein, 1970). We show such lines only when the composition immediately above or below the line is different from the composition on the line. The lines, therefore, represent composition changes or waves. If such waves are shocks, as in all but the first wave of Figure 2a, the lines separate regions of constant composition. The time-distance diagram contains sufficient information to construct either a concentration profile (fixed t_D) or an elution history ($x_D = 1$). The concentration profile at $t_D = \frac{1}{2}$ is shown in Figure 2a for both the aqueous species and the solid $\overline{AB}$. An elution history is represented by a horizontal line on the time-distance diagram, Figure 2b. The time-distance diagram shows three distinct regions.

(1) An initial condition region (region I).

(2) A region of fully spent reagent in equilibrium with the initial amount of solid $\overline{AB}$ (region II).

(3) A region of injected conditions (region III).

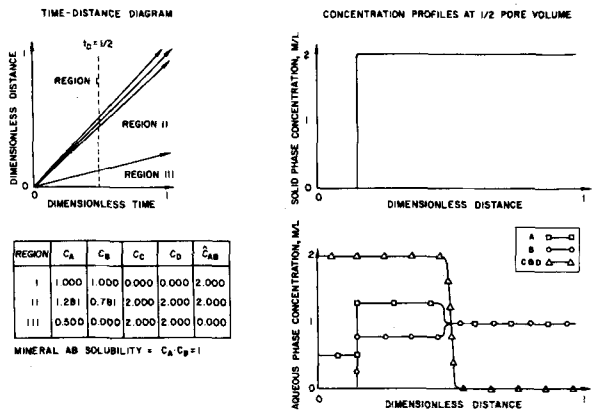

REGION	C_A	C_B	C_C	C_D	$\hat{C}_{AB}$
I	1.000	1.000	0.000	0.000	2.000
II	1.281	0.781	2.000	2.000	2.000
III	0.500	0.000	2.000	2.000	0.000

Figure 2. Time vs. distance diagram and concentration profiles at ½ pore volumes injected for *A*, *B*, *C* and *D* problem involving one solid.

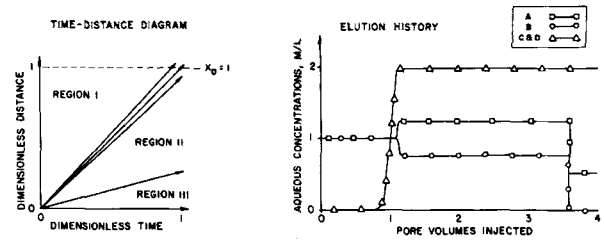

REGION	C_A	C_B	C_C	C_D	$\hat{C}_{AB}$
I	1.000	1.000	0.000	0.000	2.000
II	1.281	0.781	2.000	2.000	2.000
III	0.500	0.000	2.000	2.000	0.000

MINERAL AB SOLUBILITY = $C_A C_B = 1$

Figure 2B. Time vs. distance diagram and elution history for *A*, *B*, *C* and *D* flow problem involving one solid.

In the regions where $\overline{AB}$ is present (regions I and II), the concentrations of A and B are constrained by the solubility of the mineral.

Two waves are shown in Figure 2. The wave separating regions II and III is shown as a single line and denotes a "sharp" or "self-sharpening" wave (Helfferich and Klein, 1970). In contrast, the wave separating regions I and II is shown as a bundle of lines to denote a concentration change that is gradual which is a "spreading" wave (Helfferich and Klein, 1970). In our example, the spreading is caused by dispersion between the initial and spent solution. Although dispersion affects all waves, its effects are only pronounced when differences in fluid composition exist in regions with a constant mineral phase composition. A wave across which the fluid composition changes at constant mineral composition is a "salinity" wave.

In both regions II and III, C and D maintain their injected concentrations. In contrast, the concentrations of species A and B in region II differ from their injected concentrations, and the injected concentrations of A and B do not break through until $t_D = 3.6$ whereas C and D break through at $t_D = 1$. The species A and B are, therefore, "retarded" or move at a "retarded velocity." On a time-distance diagram, the velocity of a wave normalized by the velocity of the injected fluid—the specific velocity—is the slope of the line of the wave. The specific velocity of the unretarded salinity wave is, therefore, unity and that of the retarded wave is 0.28 (Figure 2). The concentration of all chemical species move at the same velocity; and the waves are, therefore, "coherent" (Helfferich and Klein, 1970). Based on mass balances across the shock wave, the specific wave velocity of species i is

$$v_i = \frac{1}{1 + \dfrac{\sum_{k=1}^{K} g_{ik}(\hat{C}_k^- - \hat{C}_k^+)}{\sum_{j=1}^{J} h_{ij}(C_j^- - C_j^+)}} \tag{14}$$

where the superscript + denotes upstream and − denotes downstream. The coherence condition states that the v_i are equal for all i. We will return to this point later in the paper.

For a problem involving chemical precipitation we consider, in addition to solid $\overline{AB}$, the possible formation of two new solids, $\overline{BD}$ and $\overline{AC}$ with solubility products of ½ and 2, respectively. The problem is as before with solid $\overline{AB}$ present initially and a mixture of A, C and D injected. Figure 3 shows the model calculated time-distance diagram for this example. There are now four total waves: the salinity wave (between regions I and II), two precipitation waves, and a dissolution wave (between regions IV and V). Of the two regions containing precipitates, one region contains a single precipitate, $\overline{BD}$, and the other contains two precipitates, $\overline{AC}$ and $\overline{BD}$. All waves except the salinity wave are now slowed because of either mineral dissolution or precipitation. In comparison to the previous example where C and D were transported unretarded at unit specific velocity, their injected concentrations now progress

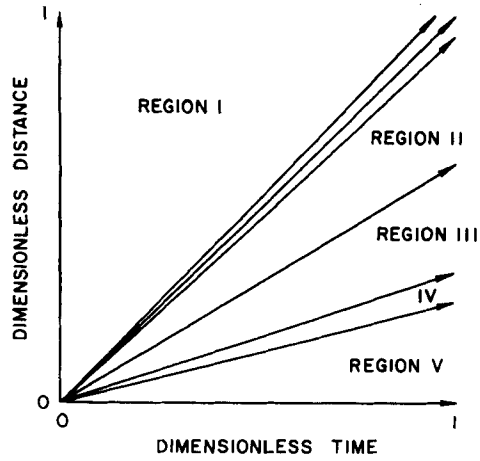

REGION	C_A	C_B	C_C	C_D	$\hat{C}_{AB}$	$\hat{C}_{AC}$	$\hat{C}_{BD}$
I	1.000	1.000	0.000	0.000	1.000	0.000	0.000
II	1.786	0.560	1.120	0.893	1.000	0.000	0.000
III	0.618	0.225	1.618	2.225	0.000	0.299	0.799
IV	0.500	0.225	1.500	2.225	0.000	0.000	0.799
V	0.500	0.000	1.500	2.000	0.000	0.000	0.000

SOLUBILITIES: $C_A \cdot C_B = 1$; $C_A \cdot C_C = 2$; $C_B \cdot C_D = 1/2$

Figure 3. Time vs. distance diagram for a four-element flow problem involving three solids.

at specific velocities of 0.23 and 0.13, respectively. In addition, the injected concentrations of A and B are also further retarded to velocities of 0.23 and 0.13, respectively, due to the precipitation.

There is an interesting consequence of the flowing equilibrium calculation manifested by the aqueous-phase concentrations in region II. The concentrations of A and B satisfy the solubility limits of solids $\overline{AC}$ and $\overline{BD}$ even though these minerals are not present in region II. This is not a coincidence but is, in fact, a general result which we have termed "the downstream equilibrium condition". This condition states that whenever a solid disappears across a wave, the downstream aqueous-phase concentrations are saturated with respect to that solid even though the solid itself is not present in the downstream region. Because the condition applies to each disappearing solid, it is not uncommon for multiple downstream equilibrium conditions to be applicable at any given time and position. For instance, in region II in Figure 3, the aqueous concentrations must be saturated with respect to the following mineral phases:

(1) Mineral $\overline{AB}$ because it is present in the region.

(2) Minerals $\overline{AC}$ and $\overline{BD}$ because the downstream equilibrium conditions apply for both these solids.

A mathematical proof of the downstream equilibrium condition is presented in the Appendix. The proof assumes the solid-phase concentration changes are step functions and concludes that all the aqueous-phase concentration changes are exponentially varying across a thin diffuse zone on the immediate upstream side of the wave. The aqueous species concentrations change in a manner that leads to the downstream equilibrium condition. Figure 10 in the Appendix illustrates the concentration profiles imposed by downstream condition. Though not applied in general, nor derived, it appears that the downstream equilibrium condition has been used by others in chromatographic transport problems (Page et al., 1975; Bunge and Radke, 1980).

We can use the coherence condition ($v_i = v$ for all i) and the downstream equilibrium condition to calculate aqueous- and solid-phase concentrations as well as wave velocities provided the correct sequence of minerals on the time-distance diagram is known. This usually requires one simulator run, but all perturbations of the injected concentration and/or the initial mineral compositions which do not alter the sequence may be calculated from this one run. This alternative to making numerous simulator runs is quite attractive since for many problems of practical interest, large amounts of computer time are required. We shall term all problems which exhibit the same mineral sequence for arbitrary changes in initial and injected conditions "scalable" problems.

The computational procedure starts with the injected aqueous-phase composition and calculates successively, in the downstream direction, the aqueous-phase compositions in adjacent regions. This can be accomplished without knowing the solid-phase compositions but does require that we know which solids are present. To calculate the solid-phase composition, given the aqueous-phase values, one must then start with the initial mineral compositions and work in the upstream direction.

Let us consider the procedure in more detail. Assume that the aqueous-phase composition (C_j^+) is known upstream of a given wave. It is desired to compute the J aqueous phase concentrations, C_j^-, in the adjacent downstream wave. There are $J - I$ intraaqueous equilibrium relations, Eq. 7 (for systems not utilizing a charge balance). If the number of different mineral phases present in both upstream and downstream region is denoted as M, there are M equilibrium relations (Eq. 9) which apply in the downstream region. Because of the downstream equilibrium condition, a solid in the upstream region results in the concentrations in the downstream region satisfying the equilibrium condition. The calculation is, therefore, the same regardless of whether a mineral appears upstream or downstream.

One other point is worth noting. Since the equilibrium relations (Eq. 9) involve only solution concentrations, the solid concentration does not enter. This is the key feature which gives rise to the algebraic solution of scalable problems.

The number of solids cannot exceed the number of elements; that is, $I \geq M$, then $J \geq M + J - I$ and additional equations are required to solve for the J unknown C_j^-.

These needed equations are provided by the coherence condition which yields $I - 1$ equations of the form:

$$v = \frac{\sum_{k=1}^{K} g_{1k}\hat{C}_k^- - \sum_{k=1}^{K} g_{1k}\hat{C}_k^+}{\sum_{j=1}^{J} h_{1j}C_j^- - \sum_{j=1}^{J} h_{1j}C_j^+} = \frac{\sum_{k=1}^{K} g_{lk}\hat{C}_k^- - \sum_{k=1}^{K} g_{lk}\hat{C}_k^+}{\sum_{j=1}^{J} h_{lj}C_j^- - \sum_{j=1}^{J} h_{lj}C_j^+} \quad \text{for } l = 2, \ldots, I \tag{15}$$

The sums extend over all possible K minerals, but only M are present. The remaining $K - M$ mineral concentrations vanish.

There will be m elements which are absent from all M minerals yielding m equations of the form:

$$\sum_{j=1}^{J} h_{ij}C_j^+ = \sum_{j=1}^{J} h_{ij}C_j^- \tag{16}$$

where i is any one of the set of m. This follows immediately from Eq. 15.

The remaining $I - m - 1$ coherence equations contain M unknown solid concentrations; they can be eliminated by algebraic manipulation leaving $I - m - M$ independent equations relating the unknown solution concentrations. We shall call this set of equations which does not contain any unknown solid concentrations, the reduced coherence conditions. There are now J equations to solve for the J unknowns. These are in summary

$J - I$ (speciation, Eq. 7)
M (solubility, Eq. 9)
m (Eq. 16)
$I - m - M$ (reduced coherence equations)

Once the solution-phase compositions are found, it is a straightforward matter to obtain the solid-phase compositions and the wave velocities using Eqs. 15 and 16. The crucial step is to begin with the known initial mineral-phase compositions which apply across the salinity wave and to calculate back toward the injection

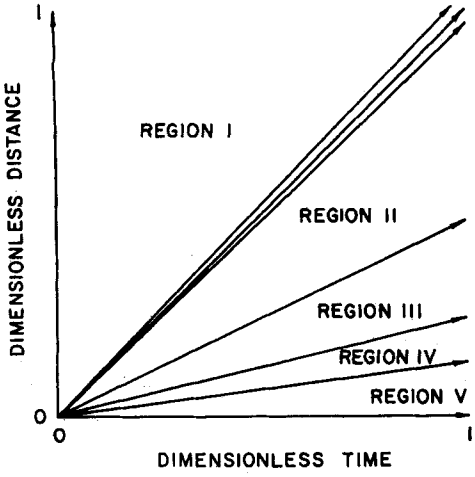

REGION	C_A	C_B	C_C	C_D	$\hat{C}_{AB}$	$\hat{C}_{AC}$	$\hat{C}_{BD}$
I	1.000	1.000	0.000	0.000	2.000	0.000	0.000
II	1.587	0.629	1.254	0.789	2.000	0.000	0.000
III	0.848	0.225	2.348	2.225	0.000	1.190	1.550
IV	0.500	0.225	2.000	2.225	0.000	0.000	1.550
V	0.500	0.000	2.000	2.000	0.000	0.000	0.000

SOLUBILITIES: $C_A \cdot C_B = 1$; $C_A \cdot C_C = 2$; $C_B \cdot C_D = 1/2$

Figure 4. Time vs. distance diagram calculated using the scaling procedure for an *A*, *B*, *C* and *D* flow problem.

point.

To make this consideration clearer, let us assume that the problem shown in Figure 3 is scalable and can be used to solve a new problem shown in Figure 4. Note that both the initial mineral concentration and the injected phase concentrations have been changed. If the problem is scalable, then there will be five regions; and the same solids found in each region shown on Figure 3 will be found in the corresponding regions in Figure 4.

To calculate the aqueous-phase compositions in region IV, given the fact that solid $\overline{BD}$ is the only one appearing in that region, write the following equations:

$$C_A(\text{IV}) = C_A(\text{V}) = 0.500 \text{ (since solids do not contain } A\text{, Eq. 16)}$$

$$C_C(\text{IV}) = C_C(\text{V}) = 1.500 \text{ (since solids do not contain } C\text{, Eq. 16)}$$

$$C_B(\text{IV}) \cdot C_D(\text{IV}) = \frac{1}{2} \text{ (solubility equilibrium, Eq. 9)}$$

The final equation stems from the coherence condition which requires, as shown by Eq. 15, that

$$\frac{-\hat{C}_{BD}}{C_B(\text{IV}) - C_B(\text{(V)}} = \frac{-\hat{C}_{BD}}{C_D(\text{IV}) - C_D(\text{V})}$$

or we find the reduced coherence condition as follows:

$$C_B(\text{IV}) - C_B(\text{V}) = C_D(\text{IV}) - C_D(\text{V})$$

This gives four equations for the four unknowns $C_A(\text{IV})$, $C_B(\text{IV})$, $C_C(\text{IV})$, and $C_D(\text{IV})$. The correct values are given in Figure 4.

The region III concentrations can be calculated next. Here we find

$$C_B(\text{III}) \cdot C_D(\text{III}) = \frac{1}{2} \text{ (Eq. 9)}$$

$$C_C(\text{III}) \cdot C_A(\text{III}) = 2 \text{ (Eq. 9)}$$

and from the coherence equation

$$\frac{\hat{C}_{BD}(\text{IV}) - \hat{C}_{BD}(\text{III})}{C_B(\text{IV}) - C_B(\text{III})} = \frac{\hat{C}_{BD}(\text{IV}) - \hat{C}_{BD}(\text{III})}{C_D(\text{IV}) - C_D(\text{III})}$$

leading to the reduced coherence condition:

$$C_B(\text{IV}) - C_B(\text{III}) = C_D(\text{IV}) - C_D(\text{III})$$

A similar application of the coherence condition relating A and C yields

$$C_A(\text{IV}) - C_A(\text{III}) = C_C(\text{IV}) - C_C(\text{III})$$

We, thus, have two equilibrium conditions and two reduced coherence conditions to determine the four unknown solution concentrations.

It is perhaps worthwhile to reiterate that in calculating the compositions in region II in Figure 4, one must apply the downstream equilibrium condition to solids $\overline{BD}$ and $\overline{AC}$

$$C_B(\text{II}) \cdot C_D(\text{II}) = \frac{1}{2} \text{ (Eq. 11)}$$

and

$$C_A(\text{II}) \cdot C_C(\text{II}) = 2 \text{ (Eq. 11)}$$

even though neither solid $\overline{BD}$ nor solid $\overline{AC}$ are present in region II. Without applying this condition, it is not possible to solve scalable problems algebraically.

Once all of the aqueous-phase concentrations have been established, the solid-phase concentrations can be calculated using Eq. 15, starting with the given initial solid phase compositions in region II and calculating those in region III. Given the values in region III, those in region IV can be determined. The wave velocities can then be calculated.

The set of nonlinear equations produced by this procedure may not always possess physically acceptable solutions. This can happen for two reasons:

(1) A fluid concentration in one or more of the regions may be negative

(2) The velocities of the waves may not decrease monotonically in the upstream direction.

The first condition is clearly nonphysical, and the second admits the possibility of multiple-valued concentrations (Helfferich and Klein, 1970). If upon calculating the velocities or the fluid concentrations one finds a discrepancy in either requirement, the problem is not scalable and the assumed mineral sequence incorrect. Our experience has shown that when a physical solution does exist, it corresponds to the solution obtained using finite differences. The solution appears to be unique, though we do not have a proof.

To summarize, the approach outlined here shows how one simulator run can be used to solve, at a great saving in computer time, an infinite set of associated scalable problems. One example, illustrating scalability, is shown next.

Uranium Roll Front Deposition

The term "roll front" deposits has been applied to the epigenetic accumulations of reduced uranium and other elements located along a roll-shaped interface between altered and unaltered sandstones. These ore deposits are typically a few meters thick, a few tens of meters wide, and a few kilometers, more or less, long. In shape, the deposits are crescent-like in cross section and elongate along the margins of the large tongues of the altered sandstone. Figure 5a shows a cross section of an idealized roll-front uranium deposit. The host rocks are predominantly reduced arkosic or siliceous sandstones which are interbedded with siltstones and claystones. The rocks are commonly of continental or marginal marine origin and range from late Mesozoic to late Tertiary in age. The Texas coastal plain deposits are of a roll front type.

Inasmuch as roll-front uranium deposits have broad similarities, it seems probable that the genetic processes responsible for their origin were similar. It is postulated (Hostetler and Garrels, 1962; Alder, 1974; Harshman, 1966) that the uranium-bearing solution,

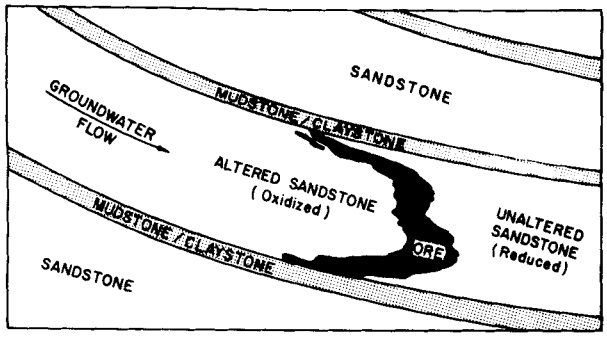

Figure 5A. Cross section of an uranium roll front showing ore distribution.

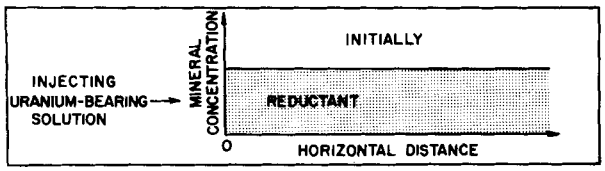

Figure 5B. One-dimensional model representation of a forming roll front in its initial stages.

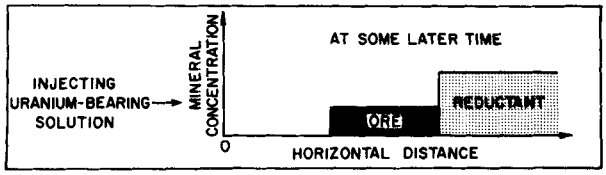

Figure 5C. One-dimensional model representation of a forming roll front at some intermediate time.

originally oxidized, migrated through porous reduced sandstone, and the uranium minerals were deposited as primary oxides. As the solution migrated down the hydraulic gradient, its oxidation potential was lowered by reaction with the indigeneous reductants; at this time the uranium oxides were precipitated from solution. The zone where the oxidation potential is lowered from its oxidized value to its reduced value is narrow. On the upstream side of the zone, an oxidative environment exists which is rich in mineralized uranium at the edge of the altered sandstone. On the downstream side of the zone, an unaltered reduced sandstone exists which typically contains pyrite (FeS_2) and organic carbon (Breger, 1974; Harshman, 1974; Hansuld, 1966; Granger and Warren, 1974). Although uraninite (UO_2), pyrite, and detrital quartz are the most frequently cited minerals in roll front deposits, numerous other minerals are also found. These minerals include coffinite ($USiO_4$), vanadium silicates, calcite, gypsum, siderite, and hematite as well as trace minerals of arsenic and selenium (Hostetler and Garrels, 1962; Harshman, 1974). To aid in the search for roll front deposits and in the production of uranium from them, much effort has been directed toward understanding the process by which uranium was deposited. For these reasons, we consider modeling the uranium

TABLE 2. MINERALS CONSIDERED IN URANIUM DEPOSITIONAL SYSTEM

FeO (ferrous oxide)	MoS_2 (molybdenite)
Fe_2O_3 (hematite)	MoO_3 (molybdite)
Fe_3O_4 (magnetite)	MoO_2
$Fe(OH)_3$ (ferric hydroxide)	$FeMoO_4$
FeOOH (goethite)	Se (selenium)
FeS_2 (pyrite)	$FeCO_3$ (siderite)
FeS (pyrrhotite)	UO_2CO_3 (rutherfordine)
$FeSO_4$ (ferrous sulfate)	As (arsenic)
UO_2 (uraninite)	As_2O_3 (arsenolite)
U_4O_9	C (carbon)
α-U_3O_8	FeAsS
$UO_2(OH)_2 \cdot H_2O$ (schoepite)	As_4O_6
α-UO_3	As_2O_5 (arsenic anhydride)
	As_2S_3 (orpiment)
	$FeSe_2$ (ferroselite)

TABLE 3. AQUEOUS SPECIES CONSIDERED IN URANIUM DEPOSITIONAL SYSTEM

H^+	U^{4+}	$HMoO_4^-$
SO_4^{2-}	$U(OH)^{3+}$	Se^{2-}
FE^{2+}	$U(OH)_2^{2+}$	HSe^{2-}
SeO_4^{2-}	$U(OH)_3^+$	O_2
UO_2^{2+}	$U(OH)_4^0$	H_2
MoO_4^{2-}	$U(OH)_5^-$	AsO_4^{3-}
OH^-	USO_4^{2+}	HCO_3^-
HS^-	UO_2^+	CO_3^{2-}
H_2S	$UO_2(OH)^+$	H_2CO_3
S^{2-}	$(UO_2)_3(OH)_5^+$	UO_2CO_3
$Fe(OH)^+$	$U(SO_4)_2$	$UO_2(CO_3)_2^{2-}$
$Fe(OH)_2$	$UO_2(SO_4)_2^{2-}$	$UO_2(CO_3)_3^{4-}$
$FeOOH^-$	UO_2SO_4	$HAsO_4^{2-}$
$FeSO_4$	Fe^{-3}	$H_2AsO_4^-$
$FeSO_4^+$	$HSeO_4^-$	AsO_2^-
$Fe(SO_4)_2^-$	H_2SeO_4	$HAsO_2$
$Fe(OH)^{2+}$	SeO_3^{2-}	AsO^+
$Fe(OH)_2^+$	$HSeO_3^-$	H_3AsO_4
$Fe(OH)_3^-$	H_2SeO_3	

depositional process. To our knowledge, no previous study along these lines has been reported.

We consider an idealized system where a high *Eh* (oxidizing) uranium-bearing groundwater contacts a porous medium containing reductants, Figures 5b and 5c. To model this system, we consider the nine most common elements: iron, uranium, sulfur, selenium, molybdenum, arsenic, carbon, hydrogen, and oxygen. Minerals derived from these elements are shown in Table 2 and the aqueous species are shown in Table 3. The solubility reactions and the solubility products of the 26 minerals at 25°C are in Table

TABLE 4. SOLUBILITY REACTIONS AND THEIR SOLUBILITY CONSTANTS AT 25°C FOR THE MINERALS IN THE URANIUM DEPOSITIONAL SYSTEM

Chemical Reaction	Logarithm of Equilibrium Constant	See Footnote
$FeO \rightleftharpoons Fe^{2+} + H_2O - 2H^+$	12.36	1
$Fe_2O_3 \rightleftharpoons 2Fe^{2+} + \frac{1}{2}O_2\uparrow - 4H^+ + 2H_2O$	−17.46	1
$Fe_3O_4 \rightleftharpoons 3Fe^{2+} + 3H_2O + \frac{1}{2}O_2\uparrow - 6H^+$	−11.79	1
$Fe(OH)_3 \rightleftharpoons Fe^{2+} + 2\frac{1}{2}H_2O + \frac{1}{4}O_2\uparrow - 2H^+$	−2.96	2
$FeOOH \rightleftharpoons Fe^{2+} + 1\frac{1}{2}H_2O + \frac{1}{4}O_2\uparrow - 2H^+$	−8.83	1
$FeS_2 \rightleftharpoons Fe^{2+} + 2SO_4^{2-} + 2H^+ - 3\frac{1}{2}O_2\uparrow$	203.96	1
$FeS \rightleftharpoons Fe^{2+} + SO_4^{2-} - 2O_2\uparrow$	126.70	1
$FeSO_4 \rightleftharpoons Fe^{2+} + SO_4^{2-}$	0.45	2
$UO_2 \rightleftharpoons UO_2^{2+} + H_2O - \frac{1}{2}O_2\uparrow - 2H^+$	27.70	3
$U_4O_9 \rightleftharpoons 4UO_2^{2+} + 4H_2O - 1\frac{1}{2}O_2\uparrow - 8H^+$	84.43	3
α-$U_3O_8 \rightleftharpoons 3UO_2^{2+} + 3H_2O - \frac{1}{2}O_2\uparrow - 6H^+$	35.02	3
$UO_2(OH)_2 \cdot H_2O \rightleftharpoons UO_2^{2+} + 3H_2O - 2H^+$	5.40	3
α-$UO_3 \rightleftharpoons UO_2^{2+} + H_2O - 2H^+$	7.69	3
$MoO_2 \rightleftharpoons MoO_4^{2-} - H_2O + 2H^+ - \frac{1}{2}O_2\uparrow$	11.59	2
$MoO_3 \rightleftharpoons MoO_4^{2-} - H_2O + 2H^+$	−12.06	2
$MoS_2 \rightleftharpoons MoO_4^{2-} - 3H_2O + 6H^+ + 2SO^{2-}{}_4$ ( ) $- 4\frac{1}{2}O_2\uparrow$	257.75	2
$FeMoO_4 \rightleftharpoons MoO_4^{2-} + Fe^{++}$	−10.45	2
$Se \rightleftharpoons SeO_4^{2-} - H_2O + 2H^+ - 1\frac{1}{2}O_2\uparrow$	35.72	2
$FeCO_3 \rightleftharpoons Fe^{2+} + CO_3^{2-}$	−12.73	4
$UO_2CO_3 \rightleftharpoons UO_2^{2+} + CO_3^{2-}$	−14.46	3
$As \rightleftharpoons AsO_4^{3-} - 1\frac{1}{2}H_2O + 3H^+ - 1\frac{1}{4}O_2\uparrow$	49.09	5
$As_2O_3 \rightleftharpoons 2AsO_4^{3-} - 3H_2O + 6H^+ - 1O_2\uparrow$	−2.75	5
$C \rightleftharpoons CO_3^{2-} - H_2O + 2H^+ - 1O_2\uparrow$	50.97	5
$FeAsS \rightleftharpoons AsO_4^{3-} + SO_4^{2-} + Fe^{2+} + 3H^+ - 1\frac{1}{2}H_2O - 3\frac{1}{4}O_2\uparrow$	184.50	6
$As_2O_5 \rightleftharpoons 2AsO_4^{3-} + 6H^+ - 3H_2O$	−38.91	6
$As_4O_6 \rightleftharpoons 4AsO_4^{3-} + 12H^+ - 6H_2O - 2O_2\uparrow$	−5.57	5
$As_2S_3 \rightleftharpoons 2AsO_4^{3-} + 3SO_4^{2-} + 12H^+ - 6H_2O - 7O_2\uparrow$	335.38	6

[1] Kharaka et al., 1973.
[2] Wagman et al., 1969.
[3] Langmuir, 1977.
[4] Wolery, 1979.
[5] Pourbaix, 1966.
[6] Robie and Waldbaum, 1968.

TABLE 5. INTRAAQUEOUS REACTIONS AND THEIR EQUILIBRIUM CONSTANTS AT 25°C FOR THE URANIUM DEPOSITIONAL SYSTEM

Chemical Reaction	Logarithm of Equilibrium Constant	See Footnote
$OH^- \rightleftharpoons H_2O - H^+$	14.00	1
$HS^- \rightleftharpoons SO_4^{2-} + H^+ - 2O_2\uparrow$	132.58	1
$H_2S \rightleftharpoons SO_4^{2-} + 2H^+ - 2O_2\uparrow$	125.59	1
$S^{2-} \rightleftharpoons SO_4^{2-} - 2O_2\uparrow$	145.51	1
$Fe(OH)^+ \rightleftharpoons Fe^{2+} + H_2O - H^+$	8.30	1
$Fe(OH)_2 \rightleftharpoons Fe^{2+} + 2H_2O - 2H^+$	17.60	1
$FeOOH^- \rightleftharpoons Fe^{2+} + 2H_2O - 3H^+$	30.70	1
$FeSO_4 \rightleftharpoons Fe^{2+} + SO_4^{2-}$	−2.43	1
$FeSO_4^+ \rightleftharpoons Fe^{2+} + SO_4^{2-} - \frac{1}{2}H_2O + H^+ + \frac{1}{4}O_2\uparrow$	−11.90	1
$Fe(SO_4)_2^- \rightleftharpoons Fe^{2+} + 2SO_4^{2-} - \frac{1}{2}H_2O + H^+ + \frac{1}{4}O_2\uparrow$	−13.15	1
$Fe(OH)_2^+ \rightleftharpoons Fe^{2+} + 1\frac{1}{2}H_2O + H^+ + \frac{1}{4}O_2\uparrow$	0.14	1
$Fe(OH)^{2+} \rightleftharpoons Fe^{2+} + \frac{1}{2}H_2O + \frac{1}{4}O_2\uparrow$	−5.59	1
$Fe(OH)_3^- \rightleftharpoons Fe^{2+} + 3H_2O - 3H^+$	31.98	1
$Fe(OH)_4^- \rightleftharpoons Fe^{2+} + 3\frac{1}{2}H_2O - 3H^+ + \frac{1}{4}O_2\uparrow$	14.24	1
$HSO_4^- \rightleftharpoons SO_4^{2-} + H^+$	−1.95	1
$U^{3+} \rightleftharpoons UO_2^{2+} - \frac{1}{2}H_2O + H^+ - \frac{3}{4}O_2\uparrow$	61.90	2
$U^{4+} \rightleftharpoons UO_2^{2+} - H_2O + 2H^+ - \frac{1}{2}O_2\uparrow$	32.33	2
$U(OH)^{3+} \rightleftharpoons UO_2^{2+} + H^+ - \frac{1}{2}O_2\uparrow$	32.99	2
$U(OH)_2^{2+} \rightleftharpoons UO_2^{2+} 1H_2O - \frac{1}{2}O_2\uparrow$	34.59	2
$U(OH)_3^+ \rightleftharpoons UO_2^{2+} + 2H_2O - H^+ - \frac{1}{2}O_2\uparrow$	37.22	2
$U(OH)_4^0 \rightleftharpoons UO_2^{2+} + 3H_2O - 2H + \frac{1}{2}O_2\uparrow$	40.88	2
$U(OH)_5^- \rightleftharpoons UO_2^{2+} + 4H_2O - 3H^+ - \frac{1}{2}O_2\uparrow$	45.49	2
$USO_4^{2+} \rightleftharpoons UO_2^{2+} + SO^{2-} - H_2O + 2H^+ - \frac{1}{2}O_2\uparrow$	26.89	2
$UO_2^+ \rightleftharpoons UO_2^{2+} + \frac{1}{2}H_2O - H^+ - \frac{1}{4}O_2\uparrow$	17.99	2
$UO_2(OH)^+ \rightleftharpoons UO_2^{2+} + H_2O - H^+$	5.78	2
$(UO_2)_3(OH)_5^+ \rightleftharpoons 3UO_2^{2+} + 5H_2O - 5H^+$	15.65	2
$UO_2SO_4 \rightleftharpoons UO_2^{2+} + SO_4^{2-}$	−2.73	2
$UO_2(SO_4)_2^- \rightleftharpoons UO_2^{2+} + 2SO_4^{2-}$	−4.25	2
$U(SO_4)_2 \rightleftharpoons UO_2^{2+} + 2SO_4^{2-} - H_2O + 2H^+ - \frac{1}{2}O_2\uparrow$	17.61	2
$Fe^{3+} \rightleftharpoons Fe^{2+} - \frac{1}{2}H_2O + H^+ + \frac{1}{4}O_2\uparrow$	−7.76	3
$HSeO_4^- \rightleftharpoons SeO_4^{2-} + H^+$	−2.04	4
$H_2SeO_4 \rightleftharpoons SeO_4^{2-} + 2H^+$	0.00	4
$SeO_3^- \rightleftharpoons SeO_4^{2-} - \frac{1}{2}O_2\uparrow$	11.79	4
$HSeO_3^- \rightleftharpoons SeO_4^{2-} + H^+ - \frac{1}{2}O_2\uparrow$	5.22	4
$H_2SeO_3 \rightleftharpoons SeO_4^{2-} + 2H^+ - \frac{1}{2}O_2\uparrow$	2.65	4
$HMoO_4^- \rightleftharpoons MoO_4^{2-} + H^+$	−6.00	3
$Se^= \rightleftharpoons SeO_4^{2-} - 2O_2\uparrow$	108.51	4
$HSe^- \rightleftharpoons SeO_4^{2-} + H^+ - 2O_2\uparrow$	94.51	4
$H_2Se \rightleftharpoons SeO_4^{2-} + 2H^+ - 2O_2\uparrow$	90.78	4
$O_2 \rightleftharpoons O_2\uparrow$	2.86	3
$H_2 \rightleftharpoons H_2O - \frac{1}{2}O_2\uparrow$	44.64	3
$HAsO_4^{2-} \rightleftharpoons AsO_4^{3-} + H^+$	−12.46	4
$H_2AsO_4^- \rightleftharpoons AsO_4^{3-} + 2H^+$	−19.72	4
$H_3AsO_4 \rightleftharpoons AsO_4^{3-} + 3H^+$	−23.30	4
$AsO_2^- \rightleftharpoons AsO_4^{3-} + 2H^+ - H_2O - \frac{1}{2}O_2\uparrow$	8.51	4
$HAsO_2 \rightleftharpoons AsO_4^{3-} - H_2O + 3H^+ - \frac{1}{2}O_2\uparrow$	−0.69	4
$AsO^+ \rightleftharpoons AsO_4^{3-} - 2H_2O + 4H^+ - \frac{1}{2}O_2\uparrow$	−0.35	4
$HCO_3^- \rightleftharpoons CO_3^{2-} + H^+$	−10.33	5
$H_2CO_3 \rightleftharpoons CO_3^{2-} + 2H^+$	−16.67	6
$UO_2CO_3 \rightleftharpoons UO_2^{2+} + CO_3^-$	−10.07	2
$UO_2(CO_3)_2^{2-} \rightleftharpoons UO_2^{2+} + 2CO_3^{2-}$	−16.98	2
$UO_2(CO_3)_3^{4-} \rightleftharpoons UO_2^{2+} + 3CO_3^{2-}$	−21.40	2

[1] Kharaka et al., 1973.
[2] Langmuir, 1977.
[3] Wagman et al., 1969.
[4] Pourbaix, 1966.
[5] Garrels and Christ, 1965.
[6] Wolery, 1979.

4. The intraaqueous reactions of the 60 aqueous species and their equilibrium constants at 25°C are shown in Table 5. Unlike the simplified problems, this problem is complicated by redox reactions. Of the nine elements considered in this system, all maintain two or more oxidation states, Table 6.

To examine the uranium deposition, ideally we would like to consider a medium consisting of a typical amount (1%) of pyrite (FeS_2) invaded by a groundwater containing a typical concentration (25 ppb) of uranium. However, such conditions would require

TABLE 6. OXIDATION STATES CONSIDERED IN URANIUM DEPOSITIONAL SYSTEM

Iron	Uranium	Sulfur	Selenium
Fe^{2+}	U^{+6}	S^{+6}	Se^{+6}
Fe^{3+}	U^{+5}	S^{+4}	Se^{+4}
	U^{+4}	S^{+2}	Se^{2-}
	U^{+3}	S^0	Se^0
		Se^{2-}	
Arsenic	**Molybdenum**	**Carbon**	**Oxygen**
As^{5+}	Mo^{+6}	C^{+4}	O^{2-}
As^{+3}	Mo^{+4}	C^0	O^0
As^0			
Hydrogen			
H^+			
H^0			

tens of thousands of pore volumes of uranium-bearing groundwater to be percolated through the reductant zone to generate a typical ore deposit. Such a simulation is not feasible with the finite difference model. We can use the simulator to construct a solution scalable to the desired one which can then be obtained using the algebraic approach set forth above. We choose a greatly reduced initial pyrite concentration and a higher than normal level of uranium concentration so that fewer pore volumes of groundwater are required to form a roll front. In this way, only a few pore volumes of groundwater will be required to give us the correct sequence of minerals. Once we know the correct number and sequence of waves, the wave velocities and their corresponding concentrations can be obtained.

The time-distance diagram showing the corrected sequence of waves, their velocities, and the mineral phase profile is in Figure 6. The figure corresponds to a porous formation ($\phi = 0.33$) consisting of 99% inert material and 1% pyrite at an *Eh* of −0.08 volts being invaded by a groundwater containing 25 ppb total dissolved uranium at an Eh of 0.61 volts. Only the positions of the minerals in the mineralized zone are shown in Figure 6. The concentrations of the aqueous and mineral species are not shown. The concentration of uraninite, the most important species, will be discussed shortly. In viewing Figure 6, one should immediately note the dimensionless time scale—tens of thousands of pore volumes. Since groundwater velocities are generally limited, the depositional process takes place over an extended time period. Most significant in Figure 6 is the sequence of waves: downstream there is a region (I) of pyrite in the unaltered sandstone; progressing upstream there is a region (II) of uraninite, selenium, and hematite; next is a region (III) of selenium and hematite; and farthest upstream there is a region (IV) of only hematite. From regions I to IV the oxidation potential changes from low reduced values in the unaltered sandstone to oxidized values in the altered sandstone, as has been observed by others (Alder, 1974; Harshman, 1966; Hansuld, 1966; Breger, 1974; Granger and Warren, 1974). Furthermore, the sequence of minerals in the narrow mineralized zone, although no doubt simplified in our predictions, is similar to what has been reported by several investigators (Harshman, 1966; Breger, 1974; Harshman, 1974). Granger and Warren (1974), for instance, have

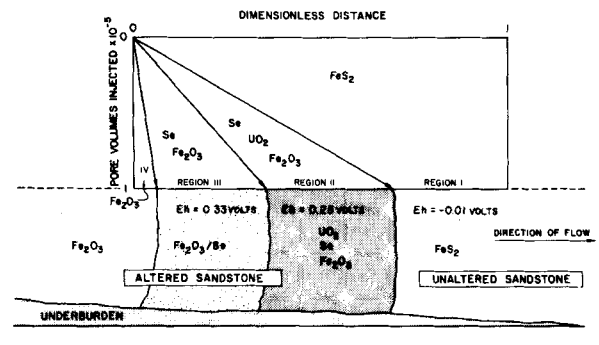

Figure 6. Model predicted time vs. distance diagram and cross section of mineralized zone for a uranium roll front. Elements used in model prediction were: Fe, U, S, Se, Mo, O, and H.

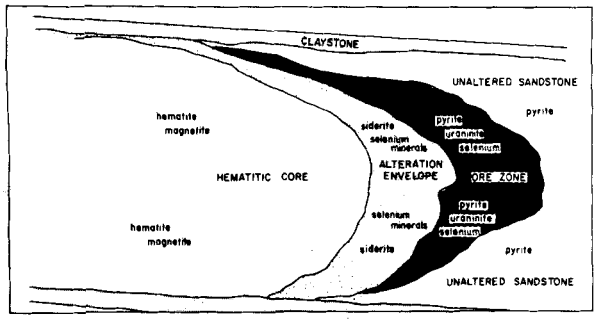

Figure 7. Idealized cross section showing minerals involved in genesis of roll-type uranium deposits as identified by Granger and Warren, 1974.

reported the results shown in Figure 7.

The model generated time-distance diagrams shown in Figure 6 is revealing in several ways. Thus far, it has been shown to determine the relative positions of minerals in the narrow mineralized zone. But, there are two other aspects which are equally as important. They are: (1) the grade of the uranium ore and (2) the age of the deposit.

Although roll front deposits of uranium are scattered widely throughout the United States, their average uranium concentration falls in a narrow range of 0.10–0.20% uranium (as U_3O_8) (DeVoto, 1978). Figure 6 gives an ore containing 0.16% uranium (U_3O_8). This grade can be altered by changing the pyrite concentration, the uranium solution concentration, or including other minerals. However, the agreement of our calculated value with those observed is an indication that the simulator may very well closely model the roll front deposition.

Unlike the uranium ore grade which can be measured, the age of a uranium deposit is uncertain (Stieff, 1953; Miller and Kulp, 1963).

From the calculations in Figure 6, the velocity of an uraninite wave can be used to estimate the time required to form an ore deposit. This will, of course, depend on the width of the deposit, the groundwater velocity, and the formation porosity. Figure 8 shows a plot of the formation time versus the width of ore zone as a function of various groundwater velocities. As the figure shows, for a 5-meter ore zone to form, it takes typically between $1\frac{1}{2}$ and 15 million years (for groundwater velocities between 0.03 and 0.30 m/yr). On the average, one might conclude that it takes about 8 million years to form an uranium ore body. This falls within the lower limit established (Dooley et al., 1964) of 250,000 years and an upper limit of about 70 million years based on the age of the host rocks (Fischer, 1968). For example, the Oakville sandstone, host of some of the South Texas deposits, is Miocene in age (7–25 million years old).

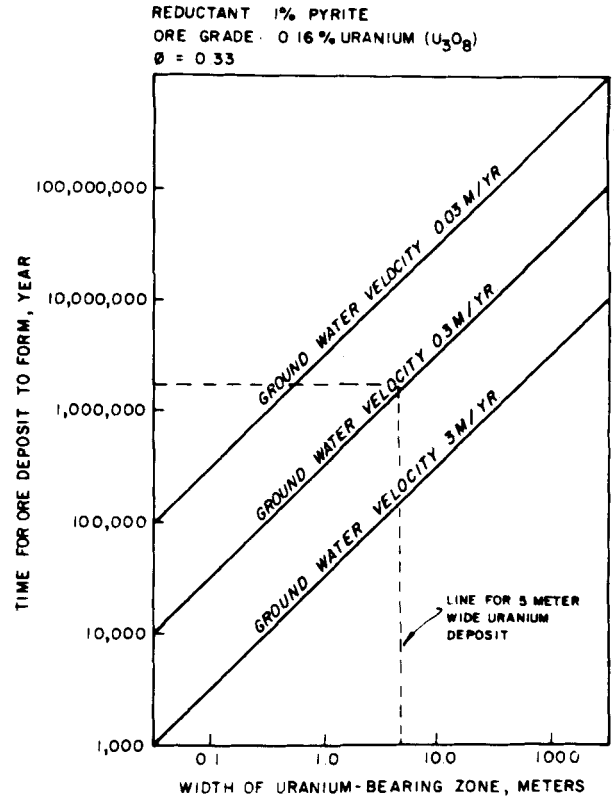

Figure 8. Time for a model-calculated roll-type uranium deposit to form.

ACKNOWLEDGMENT

The authors gratefully acknowledge the financial support of the U.S. Bureau of Mines and of the following industrial companies: Chevron Oil Field Research Co., Elf Aquitaine, Exxon Minerals Co., Everest Minerals Corp., Getty Oil Co., Halliburton Services, Marathon Resources, Inc., Phillips Petroleum Co., Rocky Mountain Energy Co., and Western Nuclear. We also thank Jon Price of The University of Texas Bureau of Economic Geology for several helpful suggestions. Schechter holds the Dula and Ernest Cockrell, Sr., Chair in Engineering.

NOTATION

a_j = chemical activity of aqueous species j
C_j = fluid-phase concentration of aqueous species j, mol/L^3
C_j^- = upstream fluid-phase concentration of aqueous species j, mol/L^3
C_j^+ = downstream fluid-phase concentration of aqueous species j, mol/L^3
$\hat{C}_k$ = solid-phase concentration of mineral k, mol/L^3
$\hat{C}_k^-$ = upstream fluid-phase concentration of aqueous species, j, mol/L^3
C_k^+ = downstream solid-phase concentration of mineral k, mol/L^3
$\hat{C}_i^T$ = total or overall concentration of element i, mol/L^3
C_{to}^T = initial total or overall concentration of element i, mol/L^3
C_{ti}^T = injected total or overall concentration of element i, mol/L^3
Eh = oxidation potential, V
F = Faraday constant, 23.06 kcal/V-g equivalent
g_{ik} = stoichiometric coefficient of the number of elements i in mineral k
G_j^o = free energy of formation of species j, kcal/gmol
h_{ij} = stoichiometric coefficient of the number of elements i in aqueous species j
$H(z)$ = Heaviside function for coordinate z
I = maximum number of elements in the system, less hydrogen and oxygen
J = maximum number of aqueous species in the system
k_i = constant of integration for component i
k_i' = constant of integration for component i
k_i'' = constant of integration for component i
k_i''' = constant of integration for component i
K = maximum number of mineral species in the system
K_{lj} = longitudinal dispersion coefficient for aqueous species j, L^2/t
K_r = equilibrium constant for intraaqueous reaction, r
K_k^{sp} = equilibrium constant for solubility reaction, k
m = number of elements not present in the different mineral phases immediately upstream or downstream of a wave
M = total number of different mineral phases present upstream and downstream of a wave
N_{Pe} = Peclet number; dimensionless dispersion coefficient
P_i^M = maximum valence or oxidation state of element i
P_{ij} = oxidation state of element i in aqueous species j
$\hat{P}_{ik}$ = oxidation state of element i in solid species k

R = maximum number of intraaqueous reactions
R_{gas} = gas constant; 1.987 kcal/gmol·K
t = time, t
t_D = dimensionless time; cumulative injection (pore volume)
T = absolute temperature, K
u = bulk aqueous-phase superficial velocity, L/t
v = bulk aqueous phase interstitial velocity (u/ϕ), L/t
v_i = specific velocity of species i
v_f = velocity of mineral precipitation wave
x = linear position, L
x_D = dimensionless position
z = moving horizontal coordinate
z_j = charge of aqueous species j
z_D = dimensionless distance for moving coordinate z

Greek Letters

$\delta(z)$ = Dirac delta function for coordinate z
ΔG_r^o = standard free-energy change of reaction for reaction r, kcal/gmol
γ_j = activity coefficient for aqueous species j
ν_{rj} = stoichiometric reaction coefficient for species j in reaction r
ϕ = porosity
ψ = concentration of available electrons in the aqueous phase
$\hat{\psi}$ = concentration of available electrons in the solid phase
ψ^T = total or overall concentration of available electrons
ψ_o^T = injected total or overall concentration of available electrons
ψ_I^T = initial total or overall concentration of available electrons

LITERATURE CITED

Adler, H. H., "Concepts of Uranium-Ore Formation in Reducing Environments in Sandstones and Other Sediments," *Proc., Symp. on the Formation of Uranium Ore Deposits, Int. Atomic Energy Agency*, Athens, Greece (May 6–10, 1974).

Bos, M., and H. Q. Meershoer, "A Computer Program for the Calculation of Equilibrium Concentrations in Complex Systems," *Anal. Chem. Acta 61* p. 185 (1972).

Breger, I. A., "The Role of Organic Matter in the Accumulation of Uranium," *Proc., Symp. on the Formation of Uranium Ore Deposits, Int. Atomic Energy Agency*, Athens, Greece (May 6–10, 1974).

Bunge, A. L., and C. J. Radke, "Migration of Alkaline Pulses in Reservoir Sands," SPE 10288, 56th Annual Fall Tech. Conf., Soc. of Pet. Eng. of AIME, San Antonio (Oct. 5–7, 1981).

Bunge, A. L., and C. J. Radke, "Divalent Ion Exchange with Alali," SPE 8995, 1980 SPE Int. Symp. on Oilfield and Geothermal Chemistry, Soc. of Pet. Eng. of AIME, Stanford University (May 28–30, 1980).

Carnahan, B., H. A. Luther, and J. O. Wilkes, *Applied Numerical Analysis*, Wiley & Sons, Inc., New York (1969).

Coats, K. H., "An Equation of State Compositional Model," *Soc. Pet. Eng. J.*, p. 363 (Oct., 1980).

Crear, P. A., "A Method of Computing Multicomponent Chemical Equilibria Based on Equilibria Constants," *Geochim. Cosochim. Acta*, **39**, p. 1375 (1975).

Davis, J. A., R. O. Janies, and J. O. Leckie, "Surface Ionization and Complexation at the Oxide/Water Interface: I. Computation of Electrical Double Layer Properties in Simple Electrolytes," *J. Colloid and Interface Sci.*, **63**(3), p. 480 (1978).

DeVoto, R. H., "Uranium Geology and Exploration," lecture notes, Colorado School of Mines, Golden, 1978.

De Zabala, E. F., J. M. Vislocky, E. Rubin, and C. J. Radke, "A Chemical Theory for Linear Alkaline Flooding," *Soc. Pet. Eng. J.*, p. 245 (April, 1982).

Dooley, Jr., J. R., M. Tatsumoto, and J. N. Rosholt, "Radioactive Disequilibrium Studies of Roll Features," *Econ. Geol.*, **59** p. 586 (1964).

Ehrlich, R., and R. J. Wygal, "Interrelation of Crude Oil and Rock Properties With the Recovery of Oil by Caustic Waterflooding," *Soc. Pet. Eng. J.*, p. 263 (Aug., 1977).

Fischer, R. P., "The Uranium and Vanadium Deposits of the Colorado Plateau Region," *Ore Deposits of the United States, 1933–1967*, J. D. Ridge, Ed. AIME, New York, **1**, p. 736 (1968).

Fleming, III, D. D., C. P. Thomas, and W. K. Winter, "Formulation of a General Multiphase, Multicomponent Chemical Flood Model," *Soc. Pet. Eng. J.*, p. 53 (Feb., 1981).

Fogler, H. S., K. Lund, and C. C. McCune, "Acidization III: The Kinetics of the Dissolution of Sodium and Potassium Feldspar in HF/HCl Mixtures," *Chem. Eng. Sci.*, **30**, p. 1325 (1975).

Gao, H. W., H. Y. Sohn, and M. E. Wadsworth, "A Mathematical Model for the In Situ Leaching of Primary Copper Ore," *Interfacing Technologies in Solution Mining*, W. J. Schlitt and J. B. Hiskey, Eds., *Proc., 2nd SME/SPE Int. Solution Mining Symp.*, Denver, (Nov. 18–20, 1981).

Garrels, R. M., and C. L. Christ, *Solutions, Minerals, and Equilibria*, Harper & Row, New York, p. 450 (1965).

Granger, H. C., and C. G. Warren, "Zoning in the Altered Tongue Associated with Roll-Type Uranium Deposits," *Proc. Symp. on the Formation of Uranium Ore Deposits, Int. Atomic Energy Agency*, Athens, Greece (May 6–10, 1974).

Hansuld, J. A., "Eh and pH in Geochemical Prospecting," *CIM&M Bull.*, **59**(647), p. 315 (1966).

Harshman, E. N., "Genetic Implications of Some Elements Associated with Uranium Deposits, Shirely Basin, Wyoming," U.S. Geol. Survey Prof, 550-C, C167 (1966).

Harshman, E. N., "Distribution of Elements in Some Roll-Type Uranium Deposits," *Proc., Symp. on the Formation of Uranium Ore Deposits, Int. Atomic Energy Agency*, Athens, Greece (May 6–10, 1974).

Hekim, Y., H. S. Fogler, and C. C. McCune, "The Radial Movement of Permeability Fronts and Multiple Reaction Zones in Porous Media," *Soc. Pet. Eng. J.*, p. 99 (Feb., 1982).

Hekim, Y., and H. S. Fogler, "On the Movement of Multiple Reaction Zones in Porous Media," *AIChE J.*, p. 403 (May, 1980).

Helfferich, F., and G. Klein, *Multicomponent Chromatography*, Marcel Dekker, Inc., New York (1970).

Helgeson, H. C., "Thermodynamics of Hydrothermal Systems at Elevated Temperatures and Pressures," *Am. J. Sci.* p. 729 (1969).

Helgeson, H. C., T. H. Brown, A. Nigrini, and T. A. Jones, "Calculation of Mass Transfer in Geochemical Processes Involving Aqueous Solutions," *Geochim. Cosochim. Acta*, **34**, p. 569 (1970).

Hill, H. J., and L. W. Lake, "Cation Exchange in Chemical Flooding: Part 3. Experimental," *Soc. Pet. Eng. J.*, p. 445 (Dec., 1978).

Himmelblau, D. M., *Applied Nonlinear Programming*, McGraw-Hill Book Co., New York (1972).

Hirasaki, G. J., "Ion Exchange with Clays in the Presence of Surfactants," *Soc. Pet. Eng. J.*, p. 181 (1982).

Hostetler, P. B., and R. M. Garrels, "Transportation and Precipitation of Uranium and Vanadium at Low Temperatures, with Special Reference to Sandstone Type Uranium Deposits," *Econ. Geol.*, **57**(2), p. 137 (1962).

I, Ting-Po, and G. H. Nancollas, "EQUIL: A Computational Method for the Calculation of Solution Equilibria," *Anal. Chem.*, **44**, p. 1940 (1972).

Ingri, N., W. Kakolowicz, L. G. Sillen, and B. Warnquist, "High Speed Computers as a Supplement of Graphical Methods—V. HALTAFALL: A General Program for Calculating the Composition of Equilibrium Mixtures," *Talanta*, **14**, p. 1261 (1967).

Kharaka, Y. K., and I. Barnes, "SOLMNEQ: Solution-Mineral Equilibrium Computations," U.S. Dept. of the Interior, Geol. Survey Computer Contr. Publ., p. 215 (1973).

Khilar, K. C., and H. S. Fogler, "Water Sensitivity of Sandstones," SPE 10103, SPE 56th Annual Fall Meeting, San Antonio (Oct., 1981).

Labrid, J. C., "Thermodynamics and Kinetic Aspects of Argillaceous Sandstone Acidizing," *Soc. Pet. Eng. J.*, p. 117 (April, 1975).

Lake, L. W., G. A. Pope, G. F. Carey, and K. Sepehrnoori, "Isothermal, Multiphase, Multicomponent Fluid Flow in Permeable Media. Part I: Description and Mathematical Formulation," Center for Enhanced Oil and Gas Recovery Research, The University of Texas at Austin (1981).

Langmuir, D., "Uranium Solution-Mineral Equilibria at Low Temperatures with Application to Sedimentary Ore Deposits," Dept. of Energy Report GJO-1659-3 (1977).

Miller, D. S., and J. L. Kulp, "Isotopic Evidence on the Origin of the Age of Some Uranium Ores of the Colorado Plateaus by the Lead-Uranium Method," U.S. Geol. Survey Cir. 271, p. 19 (1953).

Morel, F., and J. J. Morgan, "A Numerical Method for Computing Equilibria in Aqueous Chemical Systems," *Env. Sci. Tech.*, p. 58 (1972).

Page, B. W., G. Klein, F. M. Golden, and T. Vermeulen, "Mixed-Bed Ion Exchange Desalting by the Calcium Hydroxide Process," *AIChE Symp. Ser.*, **71**(152), p. 121 (1975).

Parkhurst, D. L., D. C. Thorstenson, and N. Plummer, "PHREEQE—A Computer Program for Geochemical Calculations," U.S. Geol. Survey Water Resource Invest. PB81-167801 (Nov. 1980).

Pender, H., and K. McIlwain, *Electrical Engineers Handbook*, Wiley and

Sons, New York (1950).
Perrin, D. D., and I. G. Sayce, "Computer Calculation of Equilibrium Concentrations in Mixtures of Metal Ions and Complexing Species," *Talanta*, **14**, p. 833 (1967).
Plummer, L. H., B. F. Jones, and A. H. Truesdell, "WATEQF: A Fortran IV Version of WATEQ, a Computer Program for Calculating Chemical Equilibrium of Natural Waters," U.S. Geol. Survey Water Resources Invest. 76-13 (1976).
Pope, G. A., and R. C. Nelson, "A Chemical Flooding Compositional Simulator," *Soc. Pet. Eng. J.*, p. 339 (Oct., 1978).
Pourbaix, M., *Atlas of Electrochemical Equilibria*, Pergamon Press, Inc., New York (1966).
Robinson, R. A., and R. H. Stokes, *Electrolyte Solutions*, Butterworths, London (1968).
Reed, M. G., "Gravel Peck and Formation Sandstone Dissolution During Steam Injection," *J. Pet. Tech.*, p. 941 (June, 1980).
Roache, P. J., *Computational Fluid Dynamics*, Hermose Publishers, Albuquerque (1976).
Robie, R. A., and D. R. Waldbaum, "Thermodynamic Properties of Minerals and Related Substances at 298.15 K and One Atmosphere (1.013 bars) Pressure and at Higher Temperatures," U.S. Geol. Survey Bull. No. 1259, p. 256 (1968).
Robinson, R. A., and R. H. Stokes, *Electrolyte Solutions*, Academic Press, Inc., New York (1959).
Shaughnessy, C. M., and Kunze, K. R., "Understanding Sandstone Acidizing Leads to Improved Field Practices," *J. Pet. Tech.*, p. 1196 (July, 1981).
Smith, C. F., and A. R. Hendrickson, "Hydrofluoric Acid Stimulation of Sandstone Reservoirs," *J. Pet. Tech.*, p. 215 (Feb., 1965).
Somasundran, M. E., M. Celik, A. Goyal, and E. Manev, "The Role of Surfactant Redissolution in the Adsorption of Sulfonate on Minerals," SPE 8263, 54th Annual Fall Technical Conf. and Exhibition, Las Vegas (Sept., 1979).
Stieff, L. R., T. W. Stern, and R. G. Milkey, "A Preliminary Determination of the Age of Some Uranium Ores of the Colorado Plateaus by the Lead-Uranium Method," U.S. Geol. Survey Circ. 271, p. 19 (1953).
Tatom, T. A., R. S. Schechter, and L. W. Lake, "Factors Influencing the In-Situ Acid Leaching of Uranium Ores," *Interfacing Technologies in Solution Mining*, W. J. Schlitt and J. B. Hiskey, Eds., *Proc., 2nd SME/SPE Int. Solution Mining Symp.*, Denver (Nov. 18–20, 1981).
Vetter, O. J., and V. Kandarpa, "Prediction of $CaCO_3$ Scale Under Downhole Conditions," SPE 8991, 1980 Int. Symp. on Oilfield and Geothermal Chemistry, Soc. of Pet. Eng. of the AIME, Stanford, (May 28–30, 1980).
Wagman, D. D., W. H. Evans, V. B. Parker, I. Halow, S. M. Bailey, and R. H. Schumm, "Selected Values of Chemical Thermodynamic Properties," Nat. Bureau of Standards, Technical Note 270-4 (1969).
Walsh, M. P., "Geochemical Flow Modeling," Ph.D. Dissertation, The University of Texas, at Austin (1983).
Walsh, M. P., L. W. Lake, and R. S. Schechter, "A Description of Chemical Precipitation Mechanisms and Their Role in Formation Damage During Stimulation by Hydrofluoric Acid," SPE 10625, 5th SPE Int. Symp. on Oil Field and Geothermal Chemistry, Dallas (Jan. 25–27, 1982).
Westall, J. C., J. L. Zachary, and F. M. Morel, "MINEQL: A Computer Program for the Calculation of Chemical Equilibrium Composition of Aqueous Systems," Parsons Lab. Tech. Note No. 18, Mass. Inst. of Tech., Cambridge, p. 91 (1976).
Wolery, T. J., "Calculation of Chemical Equilibrium Aqueous Solutions and Minerals," Ph.D. Dissertation, Northwestern University, Evanston, IL (1978).
Wolery, T. J., "Calculation of Chemical Equilibrium Between Aqueous Solution and Minerals: The EQ3/EQ6 Software Package," Lawrence Livermore Lab. Rept. UCRL-52658, University of California, Livermore (Feb., 1979).
Wood, C. F., "Application of 'Direct Search' to the Solution of Engineering Problems," Westinghouse Res. Lab. Sci., 6-41210-1Pl (1960).
Wylie, C. R., *Advanced Engineering Mathematics*, McGraw-Hill Book Co., New York (1966).
Zeleznik, F. J., and S. Gordon, "Calculation of Complex Chemical Equilibria," *Ind. Eng. Chem.*, **66**, p. 27 (1968).

Manuscript received August 11, 1982; revision received May 11, and accepted May 19, 1983.

APPENDIX: PROOF OF THE DOWNSTREAM EQUILIBRIUM CONDITION

The downstream equilibrium condition states that a region immediately downstream of a precipitation wave will be saturated with respect to the precipitate even though the precipitate is not present. To demonstrate this, consider the simple three element (A, B and C) problem shown in Figure 9. In a one-dimensional medium through which is flowing fluid with bulk interstitial velocity v, there exists a wave moving with an unknown velocity v_f across which solid AC is precipitating and solid AB is dissolving. The solid-phase concentrations are step functions given by

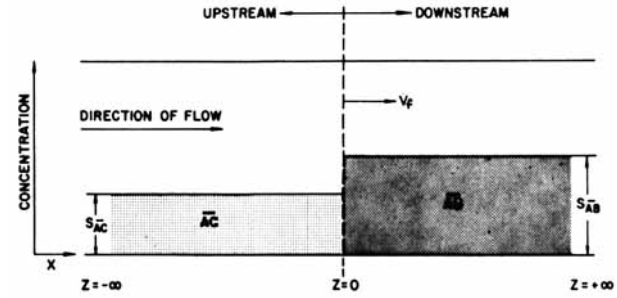

Figure 9. Schematic of a dissolution-precipitation front moving at velocity v_f. Upstream of front, precipitate $\overline{AC}$ is present; downstream of front, mineral $\overline{AB}$ is present.

$$\hat{C}_{\overline{AB}} = S_{\overline{AB}} H(z)$$

$$\hat{C}_{\overline{AB}} = S_{\overline{AC}}[1 - H(z)] \tag{17}$$

where z is a coordinate moving with the front v_f and H is the Heaviside function (Pender and McIlwain, 1950).

$$H(z) = \begin{cases} 0, & z < 0 \\ 1, & z > 0 \end{cases} \tag{18}$$

A property of the Heaviside function that we will use extensively is

$$\frac{dH(z)}{dz} = \delta(z) \tag{19}$$

where $\delta(z)$ is the Dirac delta function (Wylie, 1966).

The downstream equilibrium condition applied to this system says that

$$K \frac{SP}{\overline{AC}} = C_{\overline{A}} \cdot C_{\overline{C}} \tag{20}$$

a proposition we establish in this Appendix. The superscripts $-$ and $+$ refer to downstream and upstream positions far from the front.

The species mass balances (Eq. 1) are

$$\frac{\partial(C_i^T)}{\partial t} + v \frac{\partial C_i}{\partial x} - K_l \frac{\partial^2 C_i}{\partial x^2} = 0, \qquad i = A, B, C \tag{21}$$

and

$$C_A^T = C_A + \hat{C}_{\overline{AB}} + \hat{C}_{\overline{AC}}$$

$$C_B^T = C_B + \hat{C}_{\overline{AB}}$$

$$C_C^T = C_C + \hat{C}_{\overline{AC}} \tag{22}$$

Equation 21 may be transformed to the moving coordinate $z = x - v_f t$

$$-v_f \frac{\partial C_i^T}{\partial z} + \frac{\partial C_i^T}{\partial t} + v \frac{\partial C_i}{\partial z} - K_l \frac{\partial^2 C_i}{\partial z^2} = 0 \tag{23}$$

From our finite difference results we know that the wave will rapidly approach a constant state (Walsh et al., 1982) where it will not change shape when viewed in a moving coordinate. The time derivative in Eq. 23 is negligible, therefore, which leads to the following set of ordinary differential equations:

$$(v - v_f)\frac{dC_A}{dz} - v_f(S_{\overline{AB}} - S_{\overline{AC}})\delta(z) - K_l \frac{\partial^2 C_A}{\partial z^2} = 0$$

$$(v - v_f)\frac{dC_B}{dz} - v_f S_{\overline{AB}}\delta(z) - K_l \frac{d^2 C_B}{dz^2} = 0$$

$$(v - v_f)\frac{dC_C}{dz} + v_f S_{\overline{AC}}\delta(z) - K_l \frac{d^2 C_C}{dz^2} = 0 \tag{24}$$

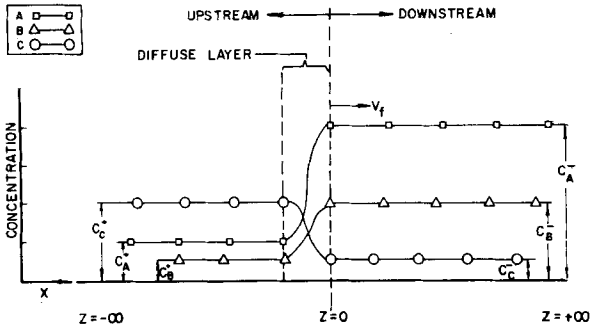

Figure 10. Corresponding aqueous phase concentrations as a function of position. The product of $C_A \cdot C_C$ equals the solubility product of $\overline{AC}$ everywhere even though $\overline{AC}$ is present only upstream.

where we have used Eqs. 17, 19 and 22. These equations may be integrated once to give

$$\frac{dC_A}{dz} = k_A e^{zD} + \frac{v_f}{K_l}(S_{\overline{AB}} - S_{\overline{AC}})e^{zD}H(z)$$

$$\frac{dC_B}{dz} = k_B e^{zD} - \frac{v_f}{K_l} S_{\overline{AB}} e^{zD}H(z)$$

$$\frac{dC_C}{dz} = k_C e^{zD} + \frac{v_f}{K_l} S_{\overline{AC}} e^{zD}H(z) \qquad (25)$$

where k_A, k_B and k_C are integration constants and $z_D = (v - v_f)$-z/K_l. A second integration yields

$$C_A = \frac{k_A K_l}{(v - v_f)} e^{zD} + \frac{v_f(S_{\overline{AB}} - S_{\overline{AC}})H(z)}{(v - v_f)}(e^{zD} - 1) + k'_A$$

$$C_B = \frac{k_B K_l}{(v - v_f)} e^{zD} - \frac{v_f S_{\overline{AB}} H(z)}{(v - v_f)}(e^{zD} - 1) + k'_B$$

$$C_C = \frac{k_C K_l}{(v - v_f)} e^{zD} + \frac{v_f S_{\overline{AC}} H(z)}{(v - v_f)}(e^{zD} - 1) + k'_C \qquad (26)$$

where k'_A, k'_B and k'_C are a second set of integration constants. We can combine constants and write out the Heaviside function explicitly to give

$$C_i = \begin{cases} k''_i e^{zD} + k'_i, & z < 0 \\ (k''_i + k'''_i)e^{zD} - k'''_i + k'_i, & z > 0 \end{cases} \qquad (27)$$

where

$$k''_i = \frac{k_i K_l}{(v - v_f)}, \quad i = A, B, C \qquad (28)$$

$$k'''_A = \frac{v_f(S_{\overline{AC}} - S_{\overline{AB}})}{(v - v_f)}$$

$$k'''_B = -\frac{v_f S_{\overline{AB}}}{(v - v_f)}$$

$$k'''_C = -\frac{v_f S_{\overline{AC}}}{v - v_f} \qquad (29)$$

We require a finite solution for z or z_D large; hence,

$$k''_i + k'''_i = 0, \quad i = A, B, C \qquad (30)$$

Furthermore, from the conditions at $z \to \pm\infty$ we gave

$$k'_i = C_i^+ \text{ and } k'_i - k'''_i = C_i^-, \quad i = A, B, C \qquad (31)$$

These conditions substituted into Eq. 33 give

$$C_i = \begin{cases} (C_i^- - C_i^+)e^{zD} + C_i^+, & z < 0 \\ C_i^-, & z > 0 \end{cases} \qquad (32)$$

Figure 10 shows the schematic profiles of Eq. 32. Now since $\overline{AC}$ is present for $z < 0$ we have

$$C_A C_C = K\frac{sp}{AC}, \quad z < 0 \qquad (33)$$

Substituting C_A and C_C into Eq. 33 from Eq. 32 and taking the limit as $z \to 0$ results in the downstream equilibrium condition, Eq. 20. Note that the C_i are constant for $z > 0$ but vary exponentially for $z < 0$. This means that a similar constraint does not apply on a region upstream of a dissolution wave as the reader may verify by applying the above procedure to the solid AB.

Fractionation with Condensation and Evaporation in Wetted-Wall Columns

A model is presented to describe the behavior of falling film fractionators with evaporation or condensation. Experimental measurements of vapor composition, vapor temperature and wall temperature profiles were made. Close agreement suggests that the model is applicable to both adiabatic and nonadiabatic conditions.

J. F. DAVIS, HSIEN-HSIN TUNG, and R. S. H. MAH

Department of Chemical Engineering
Northwestern University
Evanston, IL 60201

SCOPE

A distillation scheme which makes use of secondary reflux and vaporization (SRV) to enhance its thermal efficiency has shown considerable promise based on simulation results (Mah, et al., 1977; Fitzmorris and Mah, 1980). One promising physical realization of this scheme is to use a plate-fin device in which alternate and adjacent vertical channels serve as strippers and rectifiers (Mah, 1981). Because of heat transfer from the rectifying channels to the stripping channels, fractionation accompanied by condensation occurs continuously over the length of each rectifying channel. Similarly, fractionation accompanied by evaporation occurs over the length of each stripping channel. Unlike conventional distillation, the influence of a potentially large net mass flux between phases must be considered in modeling the SRV distillation scheme. Furthermore, because of the thermal coupling between the rectifier and

 J. F. Davis is now with the Department of Chemical Engineering, The Ohio State University. Correspondence concerning this paper should be addressed to R. S. H. Mah.